Article
Journal of Nanoscience and Nanotechnology
Vol. 18, 576–582, 2018
www.aspbs.com/jnn

A Simple α-Ketoglutarate Electrochemical Biosensor Based on Reduced MoS_2 Nanoparticle-Gold Nanoparticle Nanocomposite

Yadong Yu[1,†], Na Wu[2,†], Gang Peng[2,†], Tao Li[2], Ling Jiang[3,*], and He Huang[4,*]

[1]Jiangsu National Synergetic Innovation Center for Advanced Materials (SICAM), Nanjing 211800, People's Republic of China
[2]College of Biotechnology and Pharmaceutical Engineering, Nanjing Tech University, Nanjing, 211800, People's Republic of China
[3]College of Food Science and Light Industry, Nanjing Tech University, Nanjing 211800, People's Republic of China
[4]School of Pharmaceutical Sciences, Nanjing Tech University, Nanjing 211800, People's Republic of China

Convenient and sensitive methods for the detection of α-ketoglutarate (α-KG) will be beneficial for biomedical diagnosis and microbial fermentation industry. In this work, reduced MoS_2 nanoparticles (rMNs) were prepared by ultrasonication and electrochemical reduction. The rMNs were then decorated with gold nanoparticles (Au_{nano}) to fabricate rMNs-Au_{nano} nanocomposite. The glass carbon electrode modified with rMNs-Au_{nano} nanocomposite (rMNs-Au_{nano}-GCE) showed excellent electrocatalytic oxidation toward NADH with a satisfied reproducibility and exhibited linear response in the range of 38.46–214.29 μM. Moreover, the L-Glutamic dehydrogenase modified rMNs-Au_{nano}-GCE exhibited a sensitive and fast response to α-KG, with a linear response range of 11.12–52.94 μM and a detection limit of 6.25 μM. These findings will pave ways for the α-KG detection and the application of MoS_2 or other two-dimensional materials in electrochemical sensing.

Keywords: α-Ketoglutarate, MoS_2, Gold Nanoparticle, Electrochemical Sensing.

1. INTRODUCTION

α-Ketoglutarate (α-KG) is an important intermediate in tricarboxylic acid cycle, which serves as the key node to connect the carbon-nitrogen metabolism in cells.[1] An increasing number of evidences prove that α-KG is one of the critical metabolic markers in cancers, liver diseases and microbial fermentations.[2–4] Therefore, simple and sensitive methods for the detection of α-KG will be useful in biomedical diagnosis and fermentation industry. In the past decades, various methods including electrochemical approach, gas chromatography-mass spectrometry and liquid chromatography, have been developed for the quantification of α-KG.[3,5–8] Among these methods mentioned above, electrochemical detection technique has been regarded as a promising approach due to its advantages, such as high sensitivity, fast response and low-cost. However, to our knowledge, there are only a few studies which focused on the electrochemical detection of α-KG.

As a member of the two-dimensional (2D) materials, molybdenum disulfide (MoS_2) has attracted great attentions due to its ultra-thin structure and unique physical and chemical properties.[9,10] MoS_2 has wide applications in many fields, such as opto-electronics, channel materials, biomedicine and dry lubrication.[11–15] Recently, some researchers have successfully utilized single-layer MoS_2 to fabricate electrochemical sensors which showed good performances.[16–18] However, to obtain single-layer MoS_2 nanosheets, these works often used the intercalation exfoliation method which was time-consuming and needed harsh experimental condition.

In this paper, we described a convenient approach to prepare the electrochemically reduced MoS_2 nanoparticle decorated with gold nanoparticle (rMNs-Au_{nano}) nanocomposite by ultrasonication and electrochemical deposition. The glass carbon electrode modified with rMNs-Au_{nano} nanocomposite showed good performance in detecting NADH and α-KG (Fig. 1). These results not only facilitated the application of MoS_2 in sensor, but also provided new methods for the convenient and sensitive detection of NADH and α-KG.

*Authors to whom correspondence should be addressed.
†These three authors contributed equally to this work.

1533-4880/2018/18/576/007 doi:10.1166/jnn.2018.13945

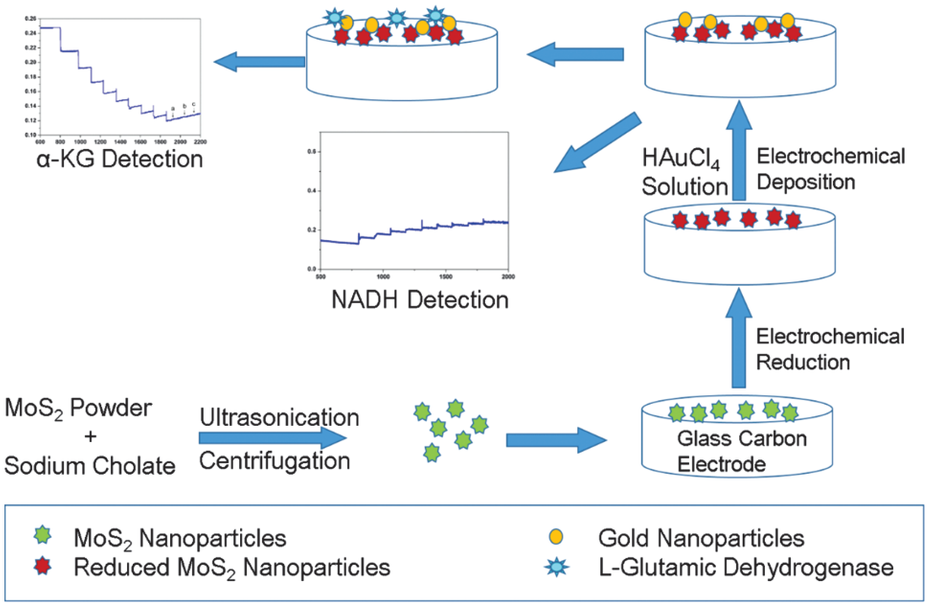

Figure 1. Schematic illustrates of reduced MoS_2 nanoparticle-based electrochemical sensors for NADH and α-KG detection.

2. MATERIALS AND METHODS

2.1. Materials and Chemicals

MoS_2 crystalline powder (<2 μm, 99%), β-nicotinamide adenine dinucleotide reduced dipotassium salt, L-Glutamic dehydrogenase (GLUD) from bovine liver-Type III and α-ketoglutaric acid sodium salt were purchased from Sigma-Aldrich Company (St. Louis, USA). Sodium cholate (98%) were obtained from Aladdin Chemistry Company (Shanghai, China). Chloroauric acid and ammonium chloride were obtained from Sinopharm Chemical Reagent Company (Shanghai, China). All other chemicals were of analytical grade and used without further purification.

2.2. Apparatus and Measurements

The glass carbon electrode (GCE) (3.0 mm diameter, CHI Instruments, Austin, USA) was polished with alumina slurry and cleaned with ethanol and DI water. Afterwards, it was activated in 0.05 M H_2SO_4 by cycling the potential from 0 to 2.0 V for seven times. All the electrochemical measurements were carried out on a CHI 650E electrochemical workstation (Chenhua Instrument Company, Shanghai, China) employing a typical three electrode cell system. A modified or bare glassy carbon electrode was utilized as the working electrode, whereas a saturated calomel electrode (SCE) as reference and a platinum foil as counter electrode. All potentials were conducted against SCE. All the experiments were purged with high-purity nitrogen to remove oxygen and done at room temperature. 0.1 M pH 7.2 phosphate buffered solution (PBS) was used as the electrolyte.

The as-prepared MoS_2 nanoparticles (MNs) were observed under a S-4800 field emission scanning electron microscopy (Hitachi, Japan). For optical absorption detection and particle size determination, the stock solution of MNs was ultrasonicated for at least 2 min and then characterized on a BIOMATE-3S UV-visible spectrophotometer (Thermo Scientific, USA) and a ZetaPALS potential analyzer (Brookhaven, USA), respectively. An X-ray diffractometer (3 kW, Rigaku Smartlab, Japan) was used to obtain the X-ray diffraction (XRD) patterns of the MNs and bulk MoS_2 powders.

2.3. Preparation of MoS_2 Nanoparticles

According to the reported method with minor modification,[19] a portion of mixed water solution, containing 2 mg/mL MoS_2 powder and 1.5 mg/mL sodium cholate, was sonicated with a JY92-IIN ultrasonic cell disruptor (Xinzhi Biotechnology Company, Ningbo, China) for 5 h. Subsequently, the resultant dispersion was centrifuged at 3000 rpm for 30 min, and then the precipitate was discarded to remove bulk MoS_2. The separated yellow–green supernatant was centrifuged at 12000 rpm for 30 min to collect MNs. To remove sodium cholate that adsorbed on the MNs, the collected MNs were further washed with ultrapure water for three times.

2.4. Preparation of Reduced MoS_2 Nanoparticle-Gold Nanoparticle Nanocomposite and NADH Electrochemical Sensor

The reduced MoS_2 nanoparticle-gold nanoparticle nanocomposite (rMNs-Au_{nano}) was prepared with electrochemical reduction and electrochemical deposition method. According to the reported method,[20] 5 μL MNs solution was dropped on GCE to prepare MNs-GCE. After dried under room temperature, the MNs-GCE was

immersed in 0.1 M PBS (pH 7.2) to conduct electrochemical reduction by applying a potential of −1.2 V for a period of 500 s. Subsequently, the resultant reduced MNs-GCE (rMNs-GCE) was put into 1 μM $HAuCl_4$ PBS solution (pH 7.2) and gold nanoparticles were electrochemically deposited (−0.2 V, 200 s) on the rMNs-GCE to obtain the gold nanoparticle decorated rMNs-GCE (rMNs-Au_{nano}-GCE). The rMNs-Au_{nano} was synthesized on the surface of GCE. After washed gently with PBS for three times and dried under room temperature, the as-prepared rMNs-Au_{nano}-GCE was used directly to detect NADH.

2.5. Preparation of α-KG Electrochemical Sensor

To prepare α-KG electrochemical sensor, 5 μL PBS containing 110 kU/L GLUD was dropped onto the surface of rMNs-Au_{nano}-GCE. After dried at 4 °C, the GLUD modified rMNs-Au_{nano}-GCE was further immersed in glutaraldehyde vapor for 3 min to form a protective film. The electrode was stored in phosphate buffer at 4 °C when it is not used.

3. RESULTS AND DISCUSSION

3.1. MoS_2 Nanoparticle Characterization

MNs were prepared by exposing bulk MoS_2 powders into ultrasonic waves in a sodium cholate solution.[19,21] As shown in Figures 2(A–B), most of the MNs showed a round-like appearance and were monodispersed. Some of the MNs were found to be aggregated, which might be caused by the lack of surfactant protection. The average diameter of the MNs was about 92.7 nm (Fig. 2(D)). As depicted in Figure 2(C), four characteristic absorption peaks (405 nm, 450 nm, 609 nm and 668 nm) were found in the as-prepared MNs samples, which were consistent with the general features of transition metal dichalcogenides with trigonal prismatic coordination and suggested the MNs were 2H polytype.[22,23] We further analyzed the XRD patterns of the MNs and bulk MoS_2 powders. We found that both the XRD patterns of the MNs and bulk MoS_2 powders showed a dominant peak at 14.4°, which suggested that the MNs and bulk MoS_2 powders were 2H MoS_2 (Fig. 3).[22] These results indicated that ultrasonication assisted-surfactant exfoliation method was an easy and efficient way to exfoliate bulk MoS_2.

3.2. Electrochemical Characterization of rMNs-Au_{nano}-GCE

Due to its intrinsically semiconducting property, MoS_2 shows the intrinsic lower electronic conductivity in comparison with graphene, which hampers its application in electrochemical sensing. Fortunately, it has been found that MoS_2 could be electrochemically reduced and the reduced MoS_2 showed good conductivity, superior electron transfer rate and high electrochemical activity.[20,24] Herein, to improve the conductivity of the MNs, we performed the electrochemical reduction treatment and optimized the reduction potential using the method reported

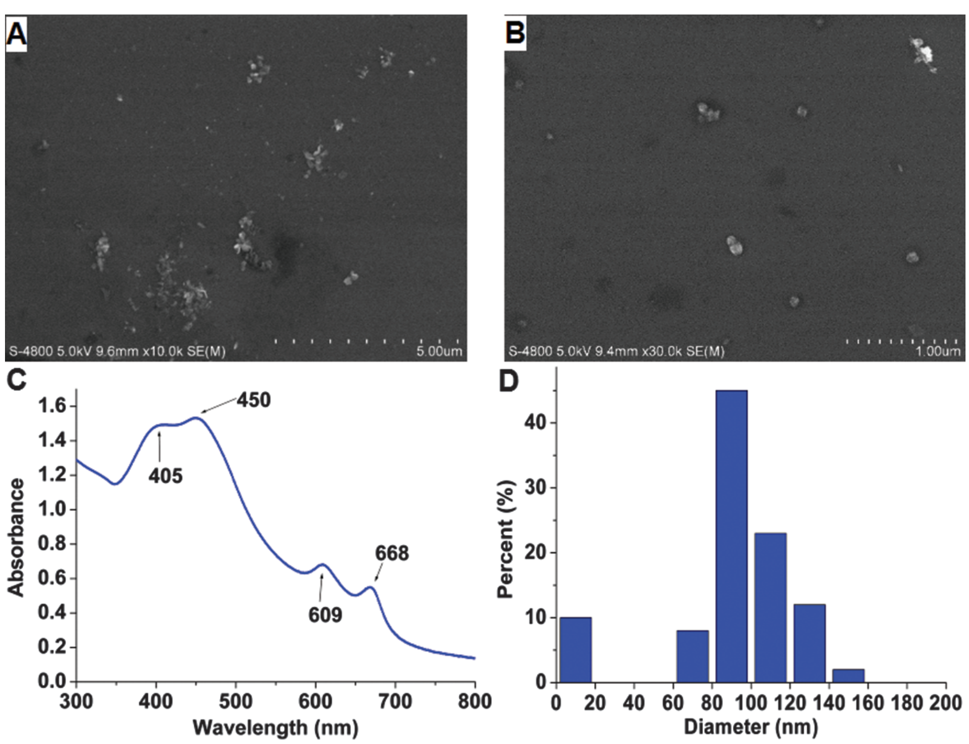

Figure 2. (A–B) SEM images of the MoS_2 nanoparticles; (C) optical absorption spectrum of the MoS_2 nanoparticle aqueous solution; (D) diameter distribution of the MoS_2 nanoparticles.

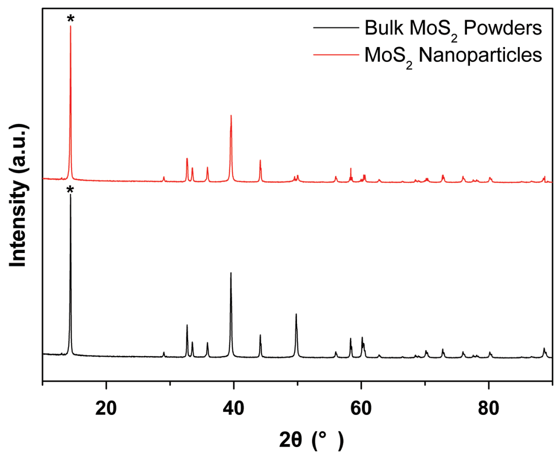

Figure 3. XRD patterns of MoS_2 nanoparticles and bulk MoS_2 powders (peaks correspond to [∗] 2H MoS_2).

by Chia et al.[20] As shown in Figure 4(A), the influence of the electrochemical reduction treatment on ΔE_p were not obvious while I_p was remarkably affected by the reduction potential. −0.8 V was the optimal reduction potential and thereby, the reduced MNs-GCE (rMNs-GCE) was prepared with electrochemical reduction at −0.8 V. Subsequently, to further enhance the signal amplification ability of the electrode, gold nanoparticles were electrochemically deposited on the rMNs-GCE. It was found that the resultant rMNs-Au_{nano}-GCE showed excellent electrochemical performances as compared with those of bare-GCE, MNs-GCE and rMNs-GCE (Fig. 4(B)).

3.3. Electrochemical Detection of NADH on rMNs-Au_{nano}-GCE

Reduced form of nicotinamide adenine dinucleotide (NADH), a pivotal coenzyme in cells, can be oxidized into its oxidized form (NAD^+) and generate electrons simultaneously. The generated electrons cause the increment of the current in the solution and thereby, various electrochemical sensors have been developed based on detecting the current changes.[25] The electrode materials with perfect electrocatalytic activity, which can reduce the oxidation potential of NADH, are necessary in detecting NADH via electrochemical approach.[25] Herein, cyclic voltammetric measurements were performed to evaluate the electrocatalytic activity of rMNs-Au_{nano}-GCE towards the oxidation of NADH. Typical cyclic voltammograms obtained for 500 μM NADH in phosphate buffer at the different modified electrodes were shown in Figure 5. The oxidation peak of NADH on the different electrodes seemed to the same (∼0.4 V). However, the oxidation peak current of NADH on rMNs-Au_{nano}-GCE was found to be the biggest as compared with those on bare-GCE, MNs-GCE, and rMNs-GCE. As shown in Figure 4(B), we compared the electrochemical properties of the MoS_2 nanoparticles (MNs), reduced MoS_2 nanoparticles (rMNs), and rMNs decorated with gold nanoparticles (rMNs-Au_{nano})

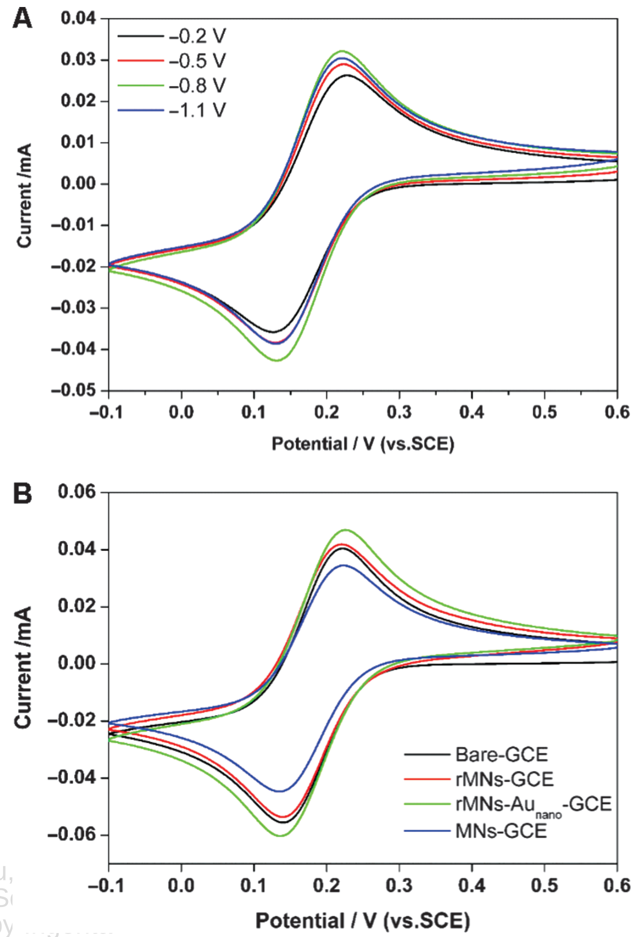

Figure 4. (A) Cyclic voltammograms of the rMNs-GCEs prepared with different reduction potentials in 5.0 mM $K_3Fe(CN)_6$ + 0.1 M KCl at a scan rate of 50 mV/s. (B) Cyclic voltammograms of the bare-GCE, rMNs-GCE, rMNs-Au_{nano}-GCE and MNs-GCE in 5.0 mM $K_3Fe(CN)_6$ + 0.1 M KCl at a scan rate of 50 mV/s.

by detecting their cyclic voltammetric (CV) responses. At the similar ΔE_p, the I_p of rMNs-Au_{nano} was significantly higher than those of bare GCE, MNs and rMNs (Fig. 4(B)). Taken together, these results suggested that the rMNs-Au_{nano} nanocomposite showed excellent electronic conductivity which favored the electron transfer between the NADH and the electrode. Moreover, as depicted in Figure 5, we found that decorating the rMNs with gold nanoparticles just enhanced the oxidation peak current of NADH, but had no significant effects on the oxidation potential. This result indicated that gold nanoparticles could improve the conductivity rather than electrocatalytic activity of the rMNs.

Based on the results shown in Figure 5, the amperometric detection of NADH was performed at 0.4 V with rMNs-Au_{nano}-GCE. Figure 6(A) showed the current-time curve for the rMNs-Au_{nano}-GCE with successive injection of NADH. The steady-state current response was attained less than 10 s. The corresponding calibration plot was presented in Figure 6(B), showing a linear response range

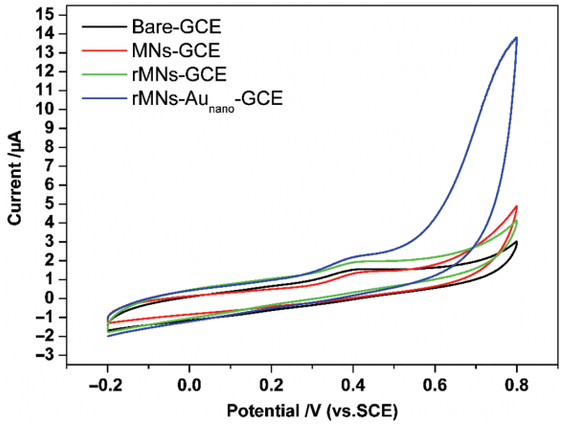

Figure 5. Cyclic voltammograms for the oxidation of 500 μM NADH at the bare-GCE, MNs-GCE, rMNs-GCE, and rMNs-Au$_{nano}$-GCE; scan rate: 50 mV/s.

from 38.46 μM to 214.29 μM and a correlation coefficient of $R^2 = 0.99838$. The calculated detection limit was 6.05 μM ($S/N = 3$). To test the reproducibility of rMNs-Au$_{nano}$-GCE, three different electrodes which were prepared with the same method were used to detect 150 μM NADH. The results showed that the relative standard deviation (RSD) was 7.1%, suggesting the as-prepared rMNs-Au$_{nano}$-GCE was reproducible.

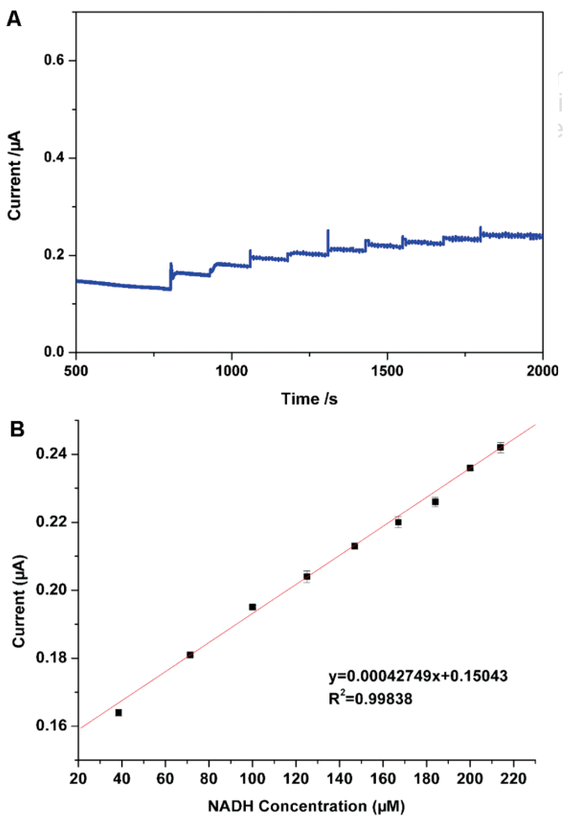

Figure 6. (A) Amperometric current-time curve recorded using the rMNs-Au$_{nano}$-GCE for successive additions of NADH; (B) the calibration curve for NADH in the range of 38.46–214.29 μM. Operating potential: 0.4 V versus SCE; rotating speed: 200 rpm.

3.4. Electrochemical Detection of α-KG on GLUD Modified rMNs-Au$_{nano}$-GCE

We further developed an amperometric biosensor for detecting α-KG based on the GLUD modified rMNs-Au$_{nano}$-GCE (GLUD-rMNs-Au$_{nano}$-GCE). The biocatalytic detection of α-KG at the GLUD-rMNs-Au$_{nano}$-GCE involves the following reaction:

$$\alpha\text{-Ketoglutarate} + NH_3 + NADH \xrightarrow{GLUD} \text{L-Glutamate} + NAD^+ + H_2O \quad (1)$$

In this reaction, GLUD catalyzes the conversion of α-KG into L-glutamate in the presence of ammonia and NADH. The quantitation of α-KG is achieved by a low-potential anodic detection of the depleted NADH at the GLUD-rMNs-Au$_{nano}$-GCE. Since NADH will be consumed by the reaction shown in Eq. (1), the remaining NADH in the solution will decrease when more α-KG is added. Consequently, the electrons generated by the oxidization of the remaining NADH at the electrode will become less and the detected currents at the electrode, which can reflect the amount of the added α-KG, will also decrease correspondingly.

Figure 7(A) displayed a typical amperometric current-time curve recorded at GLUD-rMNs-Au$_{nano}$-GCE for the successive addition of α-KG. The response time was very fast and the steady-state current response was attained less than 8 s. The linear response range at GLUD-rMNs-Au$_{nano}$-GCE was from 11.12 μM to 52.94 μM, with a correlation coefficient of -0.99242 (Fig. 7(B)). The calculated detection limit was 6.25 μM ($S/N = 3$).

To test the reproducibility of the prepared electrodes, three different GLUD-rMNs-Au$_{nano}$-GCE was prepared with the same method and studied in 0.1 M PBS containing 1 mM NADH and 1.32 mM NH_4Cl through successive addition of 66.7 μM α-KG. The results showed that the relative standard deviation was 9.2%, suggesting that the GLUD-rMNs-Au$_{nano}$-GCE was reproducible.

We further examined the effect of electroactive interferents including dopamine (DA), ascorbic acid (AA) and uric acid (UA) on the detection of α-KG at GLUD-rMNs-Au$_{nano}$-GCE. Figure 7(A) showed the amperometric responses at the GLUD-rMNs-Au$_{nano}$-GCE with the addition of different interferents. It was obvious that the presences of 0.1 mM DA, 0.1 mM AA and 0.1 mM UA have no apparent effect on the current, suggesting the as-prepared GLUD-rMNs-Au$_{nano}$-GCE showed a satisfactory anti-interference ability.

In the last decades, a variety of nanomaterials have been applied in constructing sensors.[26–38] Apart from being utilized in Li-ion batteries and other fields,[39] 2D materials such as MoS_2 also show promising potential in

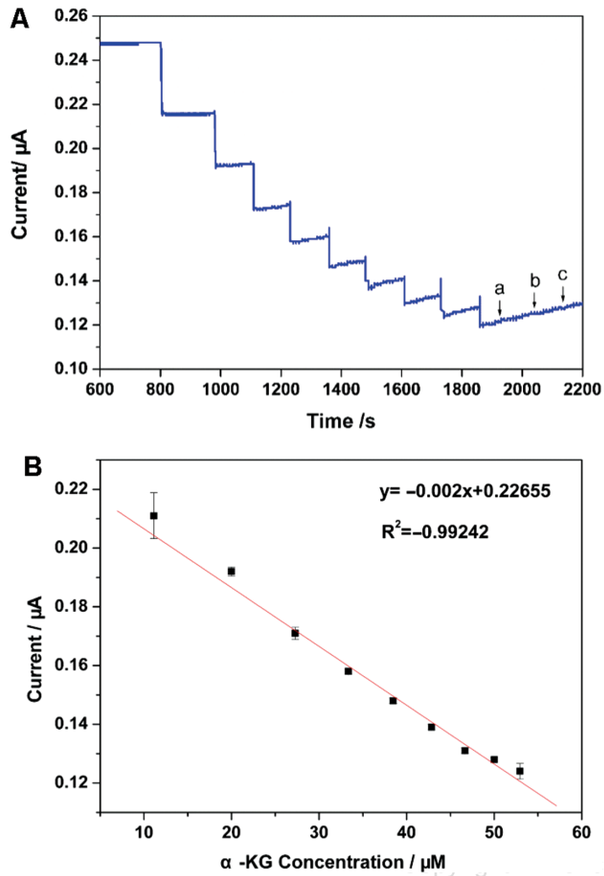

Figure 7. (A) Amperometric current-time curve recorded on the GLUD-rMNs-Au_{nano}-GCE for successive additions of α-KG; (a–c) indicated the addition of 0.1 mM DA, 0.1 mM AA and 0.1 mM UA, respectively; (B) the calibration curve for α-KG in the range of 10-60 μM. Operating potential: 0.4 V versus SCE; rotating speed: 200 rpm.

fabricating novel sensors. Herein, we demonstrated a convenient method to construct electrochemical sensors with satisfied performance. We believe that more novel sensors can be constructed by the nanocomposites which are synthesized by 2D materials and other nanomaterials in the future.

4. CONCLUSION

In this work, we provided a simple way to prepare NADH and α-KG biosensors based on rMNs-Au_{nano} nanocomposite. The prepared rMNs-Au_{nano}-GCE showed excellent electrocatalytic oxidation toward NADH with satisfied sensitivity and reproducibility. Moreover, the GLUD-rMNs-Au_{nano}-GCE exhibited a sensitive and fast response for the detection of α-KG. These findings not only provided new strategies for the electrochemical sensing of NADH and α-KG, but also showed that MoS_2 and other two-dimensional materials can be extended to construct electrochemical biosensors for biological or chemical molecules detection.

Acknowledgment: This work was financially supported by the National Science Foundation for Distinguished Young Scholars of China (No. 21225626), National Natural Science Foundation of China (No. 21506096) and National High Technology Research and Development Program of China (2013AA020302), Key Laboratory of Agro-Products Processing, Ministry of Agriculture (2015011), the State Key Laboratory of Bio-organic and Natural Products Chemistry, CAS (SKLBNPC15429), and the Six Talent Peaks Project in Jiangsu Province (2015-JY-009).

References and Notes

1. N. Wu, M. Y. Yang, U. Gaur, H. L. Xu, Y. F. Yao, and D. Y. Li, *Biomol. Ther.* 24, 1 (**2016**).
2. E. Rodriguez-Gallego, M. Guirro, M. Riera-Borrull, A. Hernandez-Aguilera, R. Marine-Casado, S. Fernandez-Arroyo, R. Beltran-Debon, F. Sabench, M. Hernandez, D. del Castillo, J. A. Menendez, J. Camps, R. Ras, L. Arola, and J. Joven, *Int. J. Obesity* 39, 279 (**2015**).
3. B. M. Wagner, F. Donnarumma, R. Wintersteiger, W. Windischhofer, and H. J. Leis, *Anal. Bioanal. Chem.* 396, 2629 (**2010**).
4. S. Zhao, Y. Lin, W. Xu, W. Jiang, Z. Zha, P. Wang, W. Yu, Z. Li, L. Gong, and Y. Peng, *Science* 324, 261 (**2009**).
5. S. Poorahong, P. Santhosh, G. V. Ramirez, T. F. Tseng, J. I. Wong, P. Kanatharana, P. Thavarungkul, and J. Wang, *Biosens. Bioelectron.* 26, 3670 (**2011**).
6. H. Terada, T. Hayashi, S. Kawai, and T. Ohno, *J. Chromatogr. A* 130, 281 (**1977**).
7. K. Michail, H. Juan, A. Maier, V. Matzi, J. Greilberger, and R. Wintersteiger, *Anal. Chim. Acta* 581, 287 (**2007**).
8. A. Collins, M. P. Nandakumar, E. Csoregi, and B. Mattiasson, *Biosens. Bioelectron.* 16, 765 (**2001**).
9. M. Chhowalla, H. S. Shin, G. Eda, L. J. Li, K. P. Loh, and H. Zhang, *Nat. Chem.* 5, 263 (**2013**).
10. V. P. Pham and G. Y. Yeom, *Adv. Mater.* 28, 9024 (**2016**).
11. L. A. King, W. J. Zhao, M. Chhowalla, D. J. Riley, and G. Eda, *J. Mater. Chem. A* 1, 8935 (**2013**).
12. Q. H. Wang, K. Kalantar-Zadeh, A. Kis, J. N. Coleman, and M. S. Strano, *Nat. Nanotechnol.* 7, 699 (**2012**).
13. D. J. Late, Y.-K. Huang, B. Liu, J. Acharya, S. N. Shirodkar, J. Luo, A. Yan, D. Charles, U. V. Waghmare, V. P. Dravid, and C. N. R. Rao, *ACS Nano* 7, 4879 (**2013**).
14. X. Yang, J. Li, T. Liang, C. Ma, Y. Zhang, H. Chen, N. Hanagata, H. Su, and M. Xu, *Nanoscale* 6, 10126 (**2014**).
15. C. Lee, Q. Li, W. Kalb, X.-Z. Liu, H. Berger, R. W. Carpick, and J. Hone, *Science* 328, 76 (**2010**).
16. S. Su, H. F. Sun, F. Xu, L. H. Yuwen, C. H. Fan, and L. H. Wang, *Microchim. Acta* 181, 1497 (**2014**).
17. H. F. Sun, J. Chao, X. L. Zuo, S. Su, X. F. Liu, L. H. Yuwen, C. H. Fan, and L. H. Wang, *Rsc Adv.* 4, 27625 (**2014**).
18. P. K. Kannan, D. J. Late, H. Morgan, and C. S. Rout, *Nanoscale* 7, 13293 (**2015**).
19. B. L. Li, H. L. Zou, L. Lu, Y. Yang, J. L. Lei, H. Q. Luo, and N. B. Li, *Adv. Funct. Mater.* 25, 3541 (**2015**).
20. X. Chia, A. Ambrosi, D. Sedmidubsky, Z. Sofer, and M. Pumera, *Chem.-Eur. J.* 20, 17426 (**2014**).
21. R. J. Smith, P. J. King, M. Lotya, C. Wirtz, U. Khan, S. De, A. O'Neill, G. S. Duesberg, J. C. Grunlan, G. Moriarty, J. Chen, J. Z. Wang, A. I. Minett, V. Nicolosi, and J. N. Coleman, *Adv. Mater.* 23, 3944 (**2011**).
22. Y. Wang, J. Z. Ou, S. Balendhran, A. F. Chrimes, M. Mortazavi, D. D. Yao, M. R. Field, K. Latham, V. Bansal, J. R. Friend,

S. Zhuiykov, N. V. Medhekar, M. S. Strano, and K. Kalantar-Zadeh, *ACS Nano* 7, 10083 **(2013)**.
23. K. F. Mak, C. Lee, J. Hone, J. Shan, and T. F. Heinz, *Phys. Rev. Lett.* 105, 136805 **(2010)**.
24. S. Wu, Z. Zeng, Q. He, Z. Wang, S. J. Wang, Y. Du, Z. Yin, X. Sun, W. Chen, and H. Zhang, *Small* 8, 2264 **(2012)**.
25. S. A. Kumar and S. M. Chen, *Sensors* 8, 739 **(2008)**.
26. K. Krishnamoorthy, G. K. Veerasubramani, S. Radhakrishnan, and S. J. Kim, *J. Nanosci. Nanotechnol*. 15, 4409 **(2015)**.
27. Z. Wang, X. Yang, J. Yang, Y. Jiang, and N. He, *Anal. Chim. Acta* 862, 53 **(2015)**.
28. J. Feng, Z. Wang, B. Shen, L. Zhang, X. Yang, and N. He, *RSC Adv.* 4, 28683 **(2014)**.
29. Z. Wang, X. Yang, J. Feng, Y. Tang, Y. Jiang, and N. He, *Analyst* 139, 6088 **(2014)**.
30. X. Xiao, K. Liu, W. Wang, H. Dong, L. Xu, and Y. Deng, *J. Bionanosci.* 8, 133 **(2014)**.
31. Y. Deng, W. Wang, L. Zhang, Z. Lu, S. Li, and L. Xu, *J. Biomed. Nanotechnol*. 9, 318 **(2013)**.
32. W. Wang, Y. Deng, L. Xu, and X. He, *J. Biomed. Nanotechnol.* 9, 736 **(2013)**.
33. Y. Deng, W. Wang, C. Ma, and Z. Li, *J. Biomed. Nanotechnol.* 9, 1378 **(2013)**.
34. Y. Deng, K. Liu, Y. Liu, H. Dong, and S. Li, *J. Nanosci. Nanotechnol.* 16, 9460 **(2016)**.
35. Y. Liu, K. Liu, H. Dong, L. Zhang, Y. Deng, C. Ma, and Z. Wang, *Nanosci. Nanotechnol. Lett*. 8, 785 **(2016)**.
36. Z. Khatoon, T. Athar, H. Fouad, A. Umar, Z. A. Ansari, and S. G. Ansari, *Nanosci. Nanotechnol. Lett*. 8, 555 **(2016)**.
37. K. Eun, S. M. Yang, Y. T. Kim, S. H. Choa, III, W. Suh, and S. H. Choa, *Nanosci. Nanotechnol. Lett*. 7, 950 **(2015)**.
38. J. H. Lee, S. K. Lee, and J. H. Park, *Nanosci. Nanotechnol. Lett.* 7, 984 **(2015)**.
39. K. Shivaa, H. S. S. R. Matte, H. B. Rajendraa, A. J. Bhattacharyya, and C. N. R. Rao, *Nano Energy* 2, 787 **(2013)**.

Received: 16 August 2016. Accepted: 16 October 2016.